SCEC-ERI SUMMER SCHOOL FOR

Earthquake Science 2014

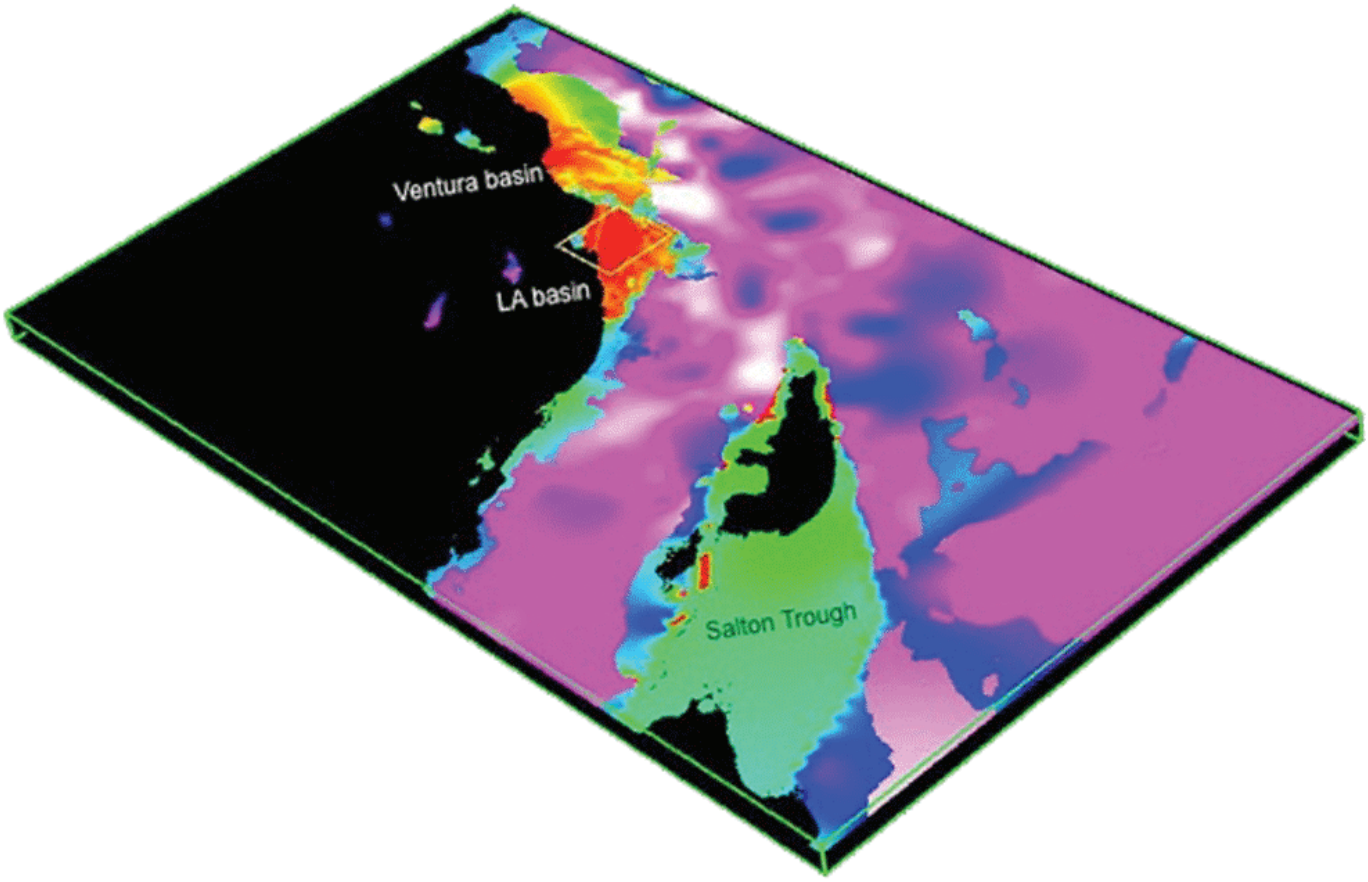

Wave and Rupture Propagation with Realistic Velocity Structures

September 28 - October 2, 2014

Oxnard, California

The **Virtual Institute for the Study of Earthquake Systems (VISES)** is a partnership between SCEC, ERI, and DPRI to develop system-level models of earthquake processes useful for risk-mitigation and resilience building in both California and Japan.

VISES is funded by a grant from the National Science Foundation's Science Across Virtual Institutes (SAVI) Program.

Southern California Earthquake Center
University of Southern California, USA

Earthquake Research Institute
The University of Tokyo, Japan

Disaster Prevention Research Institute
Kyoto University, Japan

Table of Contents

Overview

The Southern California Earthquake Center (SCEC) and the Earthquake Research Institute of the University of Tokyo (ERI) has organized a Summer School for Earthquake Science September 28 through October 2, 2014. The theme for the Summer School will be "Wave and Rupture Propagation with Realistic Velocity Structures". The program will include both lectures and exercises where participants will learn how complex velocity structure is represented and can be used to create seismograms from kinematic representations of earthquakes as point sources and propagating ruptures. One objective will be for participants to construct ground motions for earthquake scenarios, which if used in a collective sense can be a method for complementing or creating hazard maps. Participants will be given exercises so that they can run the various numerical methods with the supervision of the lecturers. Each participant will be expected to present a poster to share his/her research during evening sessions.

Participants

A total of 50 people will participate in the SCEC-ERI Summer School for Earthquake Science, including 32 students from around the world.

Organizing Committee

Ralph Archuleta, UC Santa Barbara

John Shaw, Harvard

Hiroe Miyake, ERI / U of Tokyo, Japan

Jim Mori, DPRI / Kyoto U, Japan

Tom Jordan, SCEC / USC

Greg Beroza, SCEC / Stanford

Tran Huynh, SCEC / USC

Lecturers and Instructors

Domniki Asimaki, Caltech

Jorge Crempien, UC Santa Barbara

David Gill, SCEC/USC

Rob Graves, U.S. Geological Survey

Muneo Hori, ERI / U of Tokyo, Japan

Tom Jordan, SCEC / USC

Phil Maechling, SCEC / USC

Kevin Milner, SCEC / USC

Hiroe Miyake, ERI / U of Tokyo, Japan

Jim Mori, DRPI / Kyoto U, Japan

Kim Olsen, SDSU

Andreas Plesch, Harvard

John Shaw, Harvard

Peter Shearer, UC San Diego

Fabio Silva, SCEC / USC

Rumi Takedatsu, SDSU

Students

Ryoichiro Agata, ERI / U of Tokyo, Japan

Naofumi Aso, EPS / U of Tokyo, Japan

Aida Azari Sisi, METU, Turkey

Nenad Bijelić, Stanford

Daniel Bowden, Caltech

Samuel Bydlon, Stanford

Wenyuan Fan, UC San Diego

Jacquelyn Gilchrist, UC Riverside

Thomas Goebel, Caltech

Naoki Hatakeyama, DPRI / Kyoto U, Japan

Alexandra Hutchison, UC Riverside

Naeem Khoshnevis, U of Memphis

Ryota Kiuchi, DPRI / Kyoto U, Japan

Men-Andrin Meier, Swiss Seismological Service, ETH Zurich, Switzerland

Lingsen Meng, UC Los Angeles

Kevin Milner, SCEC / USC

Irene Molinari, INGV Rome, Italy

Ryo Okuwaki, U of Tsukuba, Japan

John (Chris) Rollins, Caltech

Valerie Sahakian, UC San Diego

Kaoru Sawazaki, NIED, Japan

Xin Song, USC

Cedric Twardzik, UC Santa Barbara

Mika Usher, U of Washington

Chris Van Houtte, U of Auckland, New Zealand

Loic Viens, ERI / U of Tokyo, Japan

Erin Wirth, U of Washington

Kyle Withers, SDSU / UC San Diego

Yifei Wu, ERI / U of Tokyo, Japan

Suguru Yabe, EPS / U of Tokyo, Japan

Tomoko Yano, NEID, Japan

Lingling Ye, UC Santa Cruz

Agenda

Sunday, September 28

15:00	Check-in Embassy Suites Mandalay Beach Hotel
18:00 - 21:00	Welcome Dinner (Mandalay Ballroom C)

Monday, September 29

07:00 - 08:30	Breakfast (Coastal Grill Restaurant)
07:30 - 08:30	Software Installation Support (Mandalay Ballroom C)
08:30 - 10:00	**Unified Structural Representation of the Southern California Crust and Upper Mantle**, Prof. John Shaw, Harvard University (Mandalay Ballroom C)
10:00 - 10:30	Break
10:30 - 12:00	**Strong-motions of the 2011Tohoku-oki Earthquake: Impact on Nuclear Power Plants**, Prof. Jim Mori, Kyoto University
12:00 - 13:00	Lunch (Coastal Grill Restaurant Sky Room)
13:00 - 14:00	Software Installation Support (Mandalay Ballroom C)
14:00 - 15:30	**Full-3D Tomography: Theory and Application to Southern California**, Prof. Tom Jordan, University of Southern California
15:30 - 18:30	Computer Exercises: 3D Structural Velocity Modeling/USR Framework
18:30 - 20:30	Group Dinner (Mandalay Ballroom B)
20:30 - 22:00	Poster Viewing

Tuesday, September 30

07:00 - 08:30	Breakfast (Coastal Grill Restaurant)
08:30 - 10:00	**Broadband Kinematic Modeling of Earthquakes**, Prof. Ralph Archuleta, University of California Santa Barbara (Mandalay Ballroom C)
10:00 - 10:30	Break
10:30 - 12:00	**The GP2014 Ground Motion Simulation Technique**, Dr. Robert Graves, U.S. Geological Survey
12:00 - 13:00	Lunch (Coastal Grill Restaurant Sky Room)
13:00 - 14:00	Free Time
14:00 - 15:30	**The SDSU Broadband Ground Motion Generation Module BBtoolbox Version 1.5**, Prof. Kim Olsen, California State University at San Diego (Mandalay Ballroom C)
15:30 - 18:30	Computer Exercises: Broadband Ground Motion Simulation I
18:30 - 20:30	Group Dinner (Mandalay Ballroom B)
20:30 - 22:00	Poster Viewing

Wednesday, October 1

07:00 - 08:30	Breakfast (Coastal Grill Restaurant)
08:30 - 10:00	**UCSB Broadband Ground Motion from Kinematic Simulated Earthquakes**, Mr. Jorge Crempien, University of California Santa Barbara (Mandalay Ballroom C)
10:00 - 10:30	Break
10:30 - 12:00	**Earthquake Back-projection Methods**, Prof. Peter Shearer, University of California San Diego
12:00 - 13:00	Lunch (Coastal Grill Restaurant Sky Room)
13:00 - 14:00	Free Time
14:00 - 15:30	**Integrated Earthquake Simulation – Program Architecture and Plugged-in Components**, Prof. Muneo Hori, ERI, University of Tokyo (Mandalay Ballroom C)
15:30 - 18:30	Computer Exercises: Broadband Ground Motion Simulation II
18:30 - 20:30	Group Dinner (Poolside)
20:30 - 22:00	Poster Viewing

Thursday, October 2

07:00 - 08:30	Breakfast (Coastal Grill Restaurant)
08:30 - 10:00	**Site Response: Translating Simulated Ground Motions into Input Time-series for Engineering Design Applications**, Prof. Domniki Asimaki, California Institute of Technology
10:00 - 11:00	Discussion
11:00	Check-out Embassy Suites Mandalay Beach Hotel

Computer Exercises

Software

The program includes a lab component, where students will work in small groups to perform several computer exercises. SCEC will provide laptops (loaded with the necessary software) for the students to share and use during these exercises. Participants are welcome and encouraged to use their own laptops for this part of the program.

We will provide the scientific software to be used in the workshop as a Virtual Box Image file. The file will need to be copied onto any computer used. The SCEC-ERI image is also available online. Copies of this file on USB disk drive will be available for installation on site.

If you decide to use your own laptop, you will need to install Virtual Box (a free download from Oracle: https://www.virtualbox.org) and then to load a virtual image containing all the required software on your computer.

Computer requirements. Windows 7/8 or a Mac OS X laptop with a recent version of the OS installed, 4GB RAM (8GB+ is definitely better!), and 50GB available on the hard drive. If your computer does not meet these minimum requirements (or if you experience problems setting up your laptop with our software), you are welcome to use/share one of our laptops.

Obtain and Install Virtual Box. If you are able, please plan to install Virtual Box on your computer before the computer exercises begin on Monday afternoon.

Instructions are also posted at SCEC wiki: https://scec.usc.edu/scecpedia/Install_Virtual_Box

1. Download the Virtual Box software from Oracle (https://www.virtualbox.org/wiki/Downloads). This software is free to use. Retrieve a version that is appropriate for the Host Operating system of the computer you want to use. If your laptop runs Mac OS X, then retrieve a version of Virtual Box for Mac OS X. If your laptop runs Windows 8, retrieve a version of Virtual Box for Windows 8. We have tested the SCEC-ERI Image with Virtual Box Version 4.2.24 and higher.
2. Follow the Virtual Box installation instructions and install Virtual Box on your computer (https://www.virtualbox.org/manual/UserManual.html). The installation procedure varies slightly based on the operating system you are using. It may require administrator permissions to install virtual box on some computers.

Technical Support. Please feel free to contact us (specifically, Fabio Silva fsilva@usc.edu) for help installing Virtual Box or the workshop software.

3D Structural Velocity Modeling / USR Framework (Monday 15:30 - 18:30)

Goal. This afternoon's exercises are designed to familiarize you with the components of 3D structural velocity models, including basin structures, faults, and velocity parameterizations. We will accomplish this using the SCEC Unified Structural Representation (USR) for southern California and two tools developed to access and use this model: SCEC VDO, and interactive 3D visualization tool, and UCVM, which allows you to extract velocity values from these models.

15:30 – 15:45 Laptop setup, virtual box instructions

15:45 - 16:15 **SCEC-VDO: Structural components**

- Basics: navigation, loading plugins and datasets
- Visualizing faults: SCEC CFM
- Visualizing geologic surfaces: Basement and Moho surfaces
- Exercise: Examining faults that affect the Basement surface

16:15 - 16:45 **SCEC-VDO: Exploring velocity models**

- Examining velocity cross-sections
- Examining velocity maps
- Exercise: Comparing velocity structures and geologic surfaces

16:45 – 17:00 Break

17:00 – 18:30 **UCVM**

- Introduction to the UCVM framework
- Plotting cross sections and maps
- Exercise: Comparing alternative velocity parameterizations
- Extracting 1-D velocity profiles
- Exercise Evaluating basin velocity structures

18:30 Conclude

SCEC Broadband Platform Exercises (Tuesday & Wednesday 15:30 - 18:30)

The SCEC Broadband Platform (BBP) is a collaborative software development project involving geoscientists, earthquake engineers, graduate students, and the SCEC Community Modeling Environment. The SCEC BBP is open-source scientific software that can generate broadband (0-100Hz) ground motions for earthquakes, integrating complex scientific modules that implement rupture generation, low and high frequency seismogram synthesis, non-linear site effects calculation, and visualization into a software system that supports easy on-demand computation of seismograms.

The Broadband Platform operates in two primary modes: validation simulations and scenario simulations. In validation mode, the Platform runs earthquake rupture and wave propagation modeling software to calculate seismograms for a well-observed historical earthquake. Then, the BBP calculates a number of goodness of fit measurements that quantify how well the model-based broadband seismograms match the observed seismograms for a certain event. Based on these results, the Platform can be used to tune and validate different numerical modeling techniques.

In scenario mode, the Broadband Platform can run simulations for hypothetical (scenario) earthquakes. In this mode, users input an earthquake description, a list of station names and locations, and a 1D velocity model for their region of interest, and the Broadband Platform software then calculates ground motions for the specified stations.

The latest release includes 5 simulation methods, 7 simulation regions covering California, Japan, and Eastern North America, the ability to compare simulation results against GMPEs, and several new data products, such as map and distance-based goodness of fit plots. As the number and complexity of scenarios simulated using the Broadband Platform increases, we have added batching utilities to substantially improve support for running large-scale simulations on computing clusters.

1. Northridge SRC file, SoCal velocity structure, 5 stations within 40 km of fault (Epicentral distance is limited so that Green's functions are computed for less time.) This fault has top of rupture at 5.0 km. Choose 5 stations that are distributed at various distances from fault and various azimuths (Figure 1).
    a. Students will compute 3-component time histories, Fourier amplitude spectrum (FAS), and response spectrum.
    b. Plot the 3-components of ground motion at each site using the data.
    c. At the same scale as part b, plot the 3-components of synthetic ground motion.
    d. Compute the FAS for each component of the data and plot on log-log scale.
    e. Compute the FAS for each component of the synthetic and plot on log-log scale.
    f. Compare response spectrum from synthetic with that from GMPE (overlay two plots).
    g. For students own homework, run a different realization of the kinematic model and compare with the results from parts c and d.

2. Northridge, but SRC file will have fault coming to the surface, SoCal velocity structure, 5 stations within 40 km of fault. The dip here should be same as that for Ex.1. However, this fault has top of rupture at 0.0 km. Students can see the difference of surface vs buried rupture.
    a. Students to compute 3 component time histories, FAS, and response spectrum at the same 5 stations chosen in Exercise 1.
    b. Compare response spectrum from synthetic with that from GMPE (overlay two plots).
    c. Compare ground motions between surface rupture (Ex. 1) and buried rupture. Plot synthetics from this exercise (Ex. 2) and those from Ex. 1 on the same plot. Use SAC.

3. Strike slip, M 6.6, SoCal velocity structure, surface rupture, 5 stations. All stations are located 20 km from the fault. Hypocenter is random.
    a. Compute 3-component time histories, FAS, and response spectrum for each station.
    b. Compare response spectrum from synthetic with that from GMPE (overlay two plots).
    c. If you have time, repeat parts a and b with a different realization.

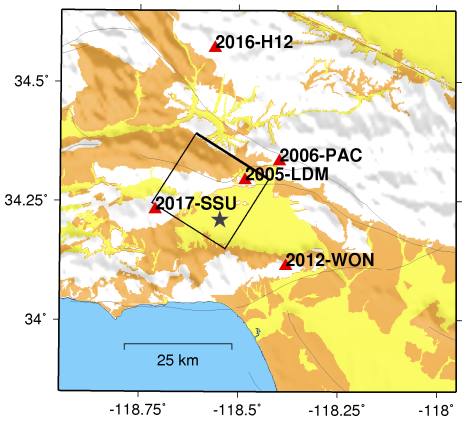

Rectangle shows the projection of the fault to the surface. The star is the location of the epicenter. The five stations for which broadband ground motions are computed.

#BBP Station List for EQID=127 (Northridge)

#Slong	Slat	RSN	Rrup (km)	Vs30 (m/s)	LoPassFre (Hz)	HiPassFreq (Hz)	Obs_File
-118.483	34.294	2005-LDM	5.9	629	0.1887	111.1111	NORTHR/2005-LDM_N.acc
-118.396	34.334	2006-PAC	7.0	2016	0.2105	111.1111	NORTHR/2006-PAC_N.acc
-118.710	34.232	2017-SSU	16.7	715	0.1263	111.1111	NORTHR/2017-SSU_N.acc
-118.380	34.114	2012-WON	20.3	1223	0.1927	111.1111	NORTHR/2012-WON_N.acc
-118.560	34.571	2016-H12	21.4	602	0.1502	111.1111	NORTHR/2016-H12_N.acc

Fault Trace with Stations

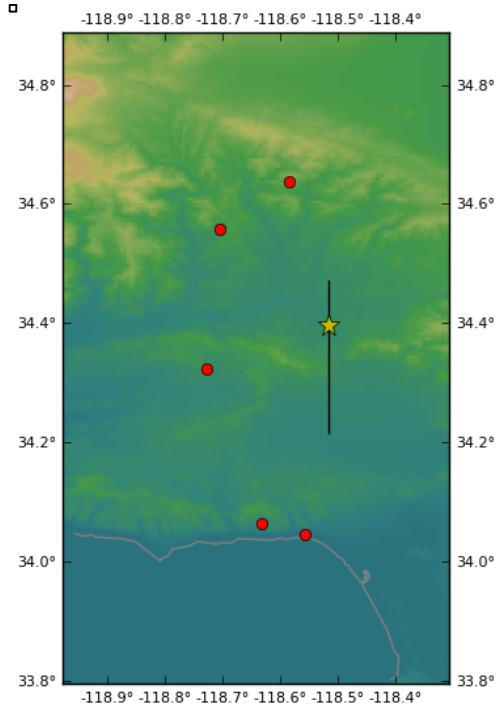

#Slon	Slat	RSN	Rrup (km)	Vs30 (m/s)
-118.631338404	34.0625956739	sta-0002	20.252155768	863
-118.704634926	34.5572255224	sta-0004	19.8543013619	863
-118.727695466	34.3234030465	sta-0016	19.5313177373	863
-118.555476883	34.0446059196	sta-0021	19.5495244908	863
-118.583951493	34.6381590417	sta-0027	19.6505388698	863

Large-scale simulation of postseismic deformation using a high-fidelity viscoelastic finite element model, *Ryoichiro Agata (ERI)*

Postseismic crustal deformation due to a subduction zone earthquake is strongly affected by the viscoelastic behavior of the asthenosphere. Several studies have used analytical or three-dimensional (3D) finite element (FE) models to simulate postseismic crustal deformation, considering the viscoelasticity. Yet because of the large computational cost, simulations using a realistic model of crustal structure have not been carried out, despite that detailed crustal data are available. Based on the technique of high performance computing, we carried out large-scale finite element simulations using 3D FE models of higher-fidelity (High-fidelity model: HFM) based on available crustal data. We constructed a one-kilometer-resolution model with the size of 3000 x 2800 x 950 km, which includes the whole of the Japanese Islands. We used the data of JTOPO30, which was constructed in a 900 m resolution by MIRC (JTOPO30, 2003), for modeling the ground surface and CAMP standard model (Hashimoto et al. 2004) for the interplate boundaries. The model has 30km thick crust and the underlying viscoelastic mantle wedge, where the Philippine Sea and the Pacific plates are subducting beneath the Eurasian and the North American plates. Since the target area was large, we also took into account the curvature of the earth. We used the K computer, the fastest super computer in Japan, for the analysis, because the degrees-of-freedom of our HFM is expected to be large.

In the session, we will show the simulation result of postseismic crustal deformation of the 2011 Tohoku-oki earthquake for 4 years using the HFM, comparing with the observation data by GEONET and Japan Coast Guard (2014).

A Parametric Study on Synthetic Uniform Hazard Spectrum of Erzincan, Turkey, *Aida Azari Sisi (METU), Aysegul Askan (METU) and Murat Altug Erberik (METU)*

In this study, stochastic earthquake catalog of Erzincan region, in Turkey is generated based on synthetic ground motions. Monte Carlo simulation method is used to identify the spatial and temporal distribution of events. The region is divided into seismic zones consisting of faults and areal sources. The magnitude distribution of zones is derived from Gutenberg-Richter recurrence model. The locations of epicenters are sampled randomly within the seismic zones. The simulations are repeated until a complete catalog is obtained. Ground motion time histories are generated for each event using stochastic simulation methods. Response spectrum of each time history is then calculated for a proper period range. Annual exceedance rate of each response is obtained from the statistical distribution of the whole response spectra for a single site. Response spectra corresponding to the same annual exceedance rate for the whole periods give site specific uniform hazard spectrum (UHS). Near-field directivity effects on UHS are then taken into account. Besides, theoretical site amplification based on transfer function is inserted into hazard calculations.

Utilization of simulated ground motions for engineering performance assessment of tall buildings, *Nenad Bijelić (Stanford), Ting Lin (Marquette), Greg Deierlein (Stanford)*

This work focuses on utilization of simulated ground motions for nonlinear structural response estimation of tall buildings. Structural building response is first estimated using conventional methods (multiple stripe analysis, incremental dynamic analysis), where recorded and simulated (broadband) ground motions are selected and scaled based on consistent hazard targets that consider spectral shape and duration. Performance demand parameters of a twenty-story building are examined at different ground motion intensity levels up to collapse to determine whether statistically significant differences exist between the responses to simulated and recorded ground motions. Amplitude scaling of both simulated and recorded ground motions is used in these analyses, following conventional approaches used in earthquake engineering. These comparisons revealed insignificant differences between the recorded and simulated ground motions, when scaled to match consistent hazard parameters. In a second on-going phase of the study, structural response is evaluated using unscaled, large-amplitude simulated ground motions generated as part of SCEC's CyberShake project. Differences in response to simulated and recorded ground motions are contrasted and opportunities and challenges for using simulated ground motions in structural performance assessment are discussed.

Observing wave propagation with ambient noise using a dense array in Long Beach, CA, *Daniel Bowden (Caltech), Victor Tsai (Caltech), Fan-Chi Lin (Univ. Utah)*

We explore a wavefront tracking methodology to recover terms for site amplification and attenuation, for use with ambient noise cross correlations. Noise cross correlations have been proven an effective means of measuring travel times between two stations, but the amplitudes of these signals is strongly biased by uneven distributions of noise sources. Because the wavefront tracking approach only observes changes in amplitude from one timestep to the next, a biased initial distribution of energy is acceptable. Changes in the wave propagation are attributed to wavefront focusing or defocusing, attenuation, sources in the array, or site amplification. The ability to observe site amplification properties at high resolution can be used to validate more traditional velocity inversions and forward modelling approaches. The approach is being tested on an extremely dense array of single component geophones in Long Beach, CA, with more than 5,000 stations.

Dynamic earthquake rupture simulations on nonplanar faults embedded in 2D and 3D geometrically complex, heterogeneous Earth models, *Sam Bydlon (Stanford), Kenneth Duru (Stanford), and Eric Dunham (Stanford)*

Dynamic propagation of shear ruptures on a frictional interface is a useful idealization of a natural earthquake. The conditions relating slip rate and fault shear strength are often expressed as nonlinear friction laws. The corresponding initial boundary value problems are both numerically and computationally challenging. In addition, seismic waves generated by earthquake ruptures must be propagated, far away from fault zones, to seismic stations and remote areas. Therefore, reliable and efficient numerical simulations require both provably stable and high order accurate numerical methods. We present a numerical method for: a) enforcing nonlinear friction laws, in a consistent and provably stable manner, suitable for efficient explicit time integration; b) dynamic propagation of earthquake ruptures along rough faults; c) accurate propagation of seismic waves in heterogeneous media with free surface topography. We solve the first order form of the 3D elastic wave equation on a boundary-conforming curvilinear mesh, in terms of particle velocities and stresses that are collocated in space and time, using summation-by-parts finite differences in space. The finite difference stencils are 6th order accurate in the interior and 3rd order accurate close to the boundaries. Boundary and interface conditions are imposed weakly using penalties. By deriving semi-discrete energy estimates analogous to the continuous energy estimates we prove numerical stability. Time stepping is performed with a 4th order accurate explicit low storage Runge-Kutta scheme. We have performed extensive numerical experiments using a slip-weakening friction law on nonplanar faults, including recent SCEC benchmark problems. We also show simulations on fractal faults revealing the complexity of rupture dynamics on rough faults. We are presently extending our method to rate-and-state friction laws and off-fault plasticity.

Kinematic earthquake rupture inversion in the frequency domain, *Wenyuan Fan (SIO/UCSD), Peter M. Shearer (SIO/UCSD) and Peter Gerstoft (SIO/UCSD)*

We develop a frequency-based approach to earthquake slip inversion that requires no prior information on the rupture velocity or slip-rate functions. Because the inversion is linear and is performed separately at each frequency, it is computationally efficient and suited to imaging the finest resolvable spatial details of rupture. We demonstrate the approach on synthetic seismograms based on the Source Inversion Validation Exercise 1 (SIV1) of a crustal Mw 6.6 strike-slip earthquake recorded locally. A robust inversion approach is obtained by applying a combination of damping, smoothing and forcing zero slip at the edge of the fault model. This approach achieves reasonable data fits, overall agreement to the SIV1 model, including slip-rate functions of each subfault, from which its total slip, slip time history and rupture velocity can be extracted. We demonstrate the method's robustness by exploring the effects of noise, random timing errors, and fault geometry errors. The worst effects on the inversion are seen from errors in the assumed fault geometry.

Possible bias in ground motion and rupture simulations arising from forced nucleation locations that are inconsistent with heterogeneous stress conditions, *Jacquelyn Gilchrist (UCR), James Dieterich (UCR), Keith Richards-Dinger (UCR) and David Oglesby (UCR)*

Initial conditions used for dynamic models, particularly the pattern of initial stresses, play a primary role in controlling rupture characteristics and resulting ground motions. We find that the location of forced rupture nucleation in models with heterogeneous initial stresses can strongly affect rupture propagation and ground motions. We use the earthquake simulator RSQSim, which is a 3D boundary element code that incorporates rate-state fault friction, to simulate long sequences of earthquakes (typically >100,000 events). We generate suites of heterogeneous initial conditions for large rupture events. In these simulations, earthquakes nucleate spontaneously — hence, each observed rupture has a set of initial stress conditions and an associated observed nucleation location that is not set a priori or forced. One important aspect of the simulations, and presumably natural fault systems, is that repeated small events (prior to a large, through-going event) test the ability of a rupture to propagate through the system at different locations, and through this process the system finds a near optimal nucleation location that enables ruptures to propagate at minimal stress conditions. Forcing nucleation at non-optimal locations for a given stress condition requires system-wide increases in shear stress to produce through-going ruptures. Compared to ruptures with heterogeneous initial stresses and arbitrary forced nucleation locations, the spontaneous RSQSim events are able to propagate at lower average initial stresses and thus have lower stress drops and lower rupture propagation speeds. Forced nucleation at other locations requires an additional 1.4 MPa of shear stress, on average, to produce a through-going rupture, but some nucleation locations require up to 3.7 MPa of additional stress. Such assumptions lead to stress drops that are, on average, 5.6 MPa, which is over 50% higher than the 3.1 MPa stress drop of the original, spontaneous event. Because the stress drops of events with forced nucleation are roughly 50% higher than the events with nucleation locations tied to the stress conditions, we expect comparable differences in the ground motions. Dynamic rupture simulations, using the finite element code FaultMod, are in progress to test this hypothesis.

A comparative study of the seismo-tectonics in the San Gorgonio and Ventura Special Fault Study Areas, *Thomas H.W. Goebel (Caltech), Egill Hauksson (Caltech), Andreas Plesch (Harvard), John H. Shaw (Harvard)*

Initial conditions used for dynamic models, particularly the pattern of initial stresses, play a primary role in controlling rupture characteristics and resulting ground motions. We find that the location of forced rupture nucleation in models with heterogeneous initial stresses can strongly affect rupture propagation and ground motions. We use the earthquake simulator RSQSim, which is a 3D boundary element code that incorporates rate-state fault friction, to simulate long sequences of earthquakes (typically >100,000 events). We generate suites of heterogeneous initial conditions for large rupture events. In these simulations, earthquakes nucleate spontaneously — hence, each observed rupture has a set of initial stress conditions and an associated observed nucleation location that is not set a priori or forced. One important aspect of the simulations, and presumably natural fault systems, is that repeated small events (prior to a large, through-going event) test the ability of a rupture to propagate through the system at different locations, and through this process the system finds a near optimal nucleation location that enables ruptures to propagate at minimal stress conditions. Forcing nucleation at non-optimal locations for a given stress condition requires system-wide increases in shear stress to produce through-going ruptures. Compared to ruptures with heterogeneous initial stresses and arbitrary forced nucleation locations, the spontaneous RSQSim events are able to propagate at lower average initial stresses and thus have lower stress drops and lower rupture propagation speeds. Forced nucleation at other locations requires an additional 1.4 MPa of shear stress, on average, to produce a through-going rupture, but some nucleation locations require up to 3.7 MPa of additional stress. Such assumptions lead to stress drops that are, on average, 5.6 MPa, which is over 50% higher than the 3.1 MPa stress drop of the original, spontaneous event. Because the stress drops of events with forced nucleation are roughly 50% higher than the events with nucleation locations tied to the stress conditions, we expect comparable differences in the ground motions. Dynamic rupture simulations, using the finite element code FaultMod, are in progress to test this hypothesis.

Study on Identification of the Physical Parameters of a Full-Scale Steel Structure Based on Observed Records, *Naoki Hatakeyama (DPRI)*

In order to predict a seismic response and subsequent damage of a building during future earthquakes, we must identify its major physical parameters, that is, shear and bending stiffness and mass of the target building. However, it is difficult to directly estimate these physical parameters. In this study, we try to identify the physical parameters of a full-scale five-storied steel structure based on the observed microtremor records in the center of all the floors. First, we estimate 1^{st} -5^{th} resonant frequencies by using Fourier spectral ratios of each floor response with respect to the ground. We then observe the changes of these resonant frequencies due to loading of an added weight with known amount (in the case of this study, 3tons) in each floor as a sequence of experiments. Finally, using an equivalent lumped mass flexural-shear model (not considering rotatory inertia) or a lumped mass flexural-shear model (considering rotatory inertia), we identify its physical parameters which minimize residuals between theory and observation of the original and shifted resonant frequencies through the Hybrid Heuristic Search method (HHS method). The HHS method is combination of Genetic Algorithm and Heuristic Search with the concept of Simulated Annealing. When we apply the lumped mass flexural-shear model, we can drastically decrease residuals in comparison to the shear model.

Systematic Search for Ambient Non-Volcanic Tremor in the San Jacinto Fault, *Alexandra A. Hutchison (UCR) and Abhijit Ghosh (UCR)*

In this exploratory study, we use seismic array data and Plate Boundary Observatory (PBO) borehole broadband seismic data to search for ambient tremor in the San Jacinto Fault (SJF) and the southern San Andreas Fault (SAF). We are particularly interested in the region surrounding the Anza Gap, an aseismic segment of the SJF that has been accumulating stress as the rest of the fault segments have undergone MW ~6+ earthquakes for the last hundred years or so (Thatcher et al., 1975; Sanders and Kanamoori, 1984), likely posing a major seismic hazard to the surrounding region. During the time period for which there is array data available—March to July, 2011—we apply a beamforming algorithm (Ghosh et al., 2009) to automatically scan for ambient tremor in the region. We compare the location of the beam in the slowness space relative to the center of the array to determine the signal's origin. Should the origin match the slowness parameters of tremor originating in the SJF or the southern SAF, we apply a set of criteria to eliminate all other possibilities, such as regular earthquakes, noise, etc. In addition, we visually check the data for a tremor-like signal and eliminate any possible artifacts. We also apply back-projection, a technique that was employed to track rupture propagation following the 2004 Sumatra-Andaman earthquake (Ishii *et al.*, 2005), to locate the candidate signals in the latitudinal-longitudinal space and determine if it corresponds to a fault, and moreover if the signal migrates as would be expected of tremor. Our preliminary analyses found some interesting tremor-like signals, which require further investigation.

Evaluation of the Southern California Velocity Models through Simulation and Validation of Multiple Historical Events, *Naeem Khoshnevis (CERI/U Memphis), Shima Azizzadehroodpish (CERI/U Memphis) and Ricardo Taborda (CERI/ U Memphis)*

We conduct a series of simulations for multiple historical moderate-magnitude earthquakes and validate our results against recorded data to evaluate the velocity models available for southern California. SCEC supports two main community velocity models for the region, namely CVM-S and CVM-H. Both models offer different possibilities or variations, which can be accessed via the SCEC UCVM Platform. CVM-S, for instance, can be queried in its original version (CVM-S4), or with modifications recently included after a 3D tomographic inversion study (CVM-S4.26). The information in CVM-H, on the other hand, can be alternatively used with a supplemental geotechnical model (GTL) or without it. One can therefore produce two different models, CVM-H+GTL (i.e., CVM-H with the GTL model) or CVM-H (i.e., without it). We performed multiple simulations of earthquakes with magnitudes varying between 3.5 and 5.5 using the four models just described (CVM-S4, CVM-S4.26, CVM-H, and CVM-H+GTL). The simulations were done for a maximum frequency of 1 Hz and a minimum shear wave velocity of 200 m/s using Hercules, an octree-based finite-element parallel earthquake ground motion simulator. The earthquake ruptures were modeled assuming a kinematic point-source (double-couple) representation. Synthetics on about 50 stations per event were compared with data recorded during the earthquakes and downloaded from the Southern California Earthquake Data Center. The seismograms were processed and compared with the synthetics in the range of 0.1--1.0 Hz using a modified version of the Anderson Goodness-of-Fit (GOF) method. This method combines various comparison criteria that are meaningful to both engineers and seismologists, and has been satisfactorily used in previous validation efforts. We compare the regional distribution of the GOF results for all the earthquakes and all the models and draw conclusions on the consistency observed in the results.

Focal Mechanism Dependence of Apparent Stress for Moderate and Large Earthquakes, *Ryota Kiuchi (DPRI/Kyoto U) and Jim Mori (DPRI/Kyoto U)*

Earthquake radiated seismic energy is defined as the total wave energy and can contribute to understanding the source physics. For large earthquakes, it is known that strike-slip events have higher radiated energy than normal and thrust ones from teleseismic P-waves (e.g., Perez-Campos and Beroza, 2001; Convers and Newman, 2011). However, estimates of radiated energy from teleseismic P-waves can be unstable due to the small values for radiation pattern with take-off angles near the nodes of the focal mechanisms. On the other hand, for small and moderate events, same dependency with large events have not been obtained ever. In this study, we explore about radiated energy dependence on focal mechanism for moderate (M~5) and large earthquakes (M>7).

For 174 large earthquakes, We use teleseismic waveform data recorded on the GSN network and the method which takes into account for depth phase pP and sP as well as direct P phase (Boatwright and Choy, 1986). In addition, we use an our improved method for radiation pattern correction (2013, AGU). It considers a range of values for the strike, dip and rake angles, because estimated focal mechanisms have uncertainty and change during the rupture progress due to the geometry of slip can be quite complicated for large earthquakes. For moderate earthquakes, we apply an empirical Green's function (EGF) method to the S-wave of regional data (less than 100km) to remove the site and path effects.

Using our improved method, estimated radiated seismic energy for large strike-slip earthquakes becomes smaller than previous study, and the standard deviation of energy also decrease. However, large strike-slip earthquakes have from 5 to 6 times larger radiated energy than dip-slip ones. In addition, we try to estimate the apparent stress for moderate events.

A Filter Bank Approach to Earthquake Early Warning, *Men-Andrin Meier (ETH Zurich), Tom Heaton (Caltech), John Clinton (ETH Zurich)*

Earthquake Early Warning (EEW) is a race against time. The longer it takes to detect and characterize an ongoing event, the larger is the blind zone - the region where a warning arrives only after the most damaging ground motion has occurred. The problem is most acute during medium size earthquakes, which can cause severe damage but where the damaging ground motion is confined to a small zone around the epicenter. An ideal EEW algorithm which is fast enough to provide relevant alerts for such scenario events would have to produce reliable event characterization based on observations of very short snippets of data recorded at only very few stations. For such a scheme to work, without significant numbers of false alarms (which continue to hamper both single-station and network based approaches today), the real-time information that is available for an earthquake has to be exploited in a more optimal way than what is currently done.

Our approach is to fully mine the broadband frequency content of incoming real-time waveforms. We propose a filter bank approach with minimum phase delay filters which allows us to use frequency information from each frequency band at each triggered station at the earliest possible time. We have compiled and processed an extensive dataset of near-field earthquake waveforms. In an empirical maximum likelihood scheme, we use the filter bank output from the first seconds after the P-wave onset of each waveform to estimate the most likely magnitude and epicentral distance to have caused this waveform. We show how our single station approach can be integrated into an evolutionary and fully probabilistic network EEW system. We demonstrate that our method can allow sufficiently accurate characterization of an ongoing event with two stations, with systematic characterization of the evolving uncertainty of the location and magnitude.

Operational earthquake forecasting in California: A prototype system combining UCERF3 and CyberShake, *Kevin R. Milner (USC), Thomas H. Jordan (USC), and Edward H. Field (USGS Golden)*

Operational earthquake forecasting (OEF) is the dissemination of authoritative information about time-dependent earthquake probabilities to help communities prepare for potentially destructive earthquakes. The goal of OEF is to inform the decisions that people and organizations must continually make to mitigate seismic risk and prepare for potentially destructive earthquakes on time scales from days to decades. To attain this goal, OEF must provide a complete description of the seismic hazard—ground motion exceedance probabilities as well as short-term rupture probabilities—in concert with the long-term forecasts of probabilistic seismic hazard analysis. We have combined the Third Uniform California Earthquake Rupture Forecast (UCERF3) of the Working Group on California Earthquake Probabilities (Field et al., 2014) with the CyberShake ground-motion model of the Southern California Earthquake Center (Graves et al., 2011; Callaghan et al., this meeting) into a prototype OEF system for generating time-dependent hazard maps. UCERF3 represents future earthquake activity in terms of fault-rupture probabilities, incorporating both Reid-type renewal models and Omori-type clustering models. The current CyberShake model comprises approximately 415,000 earthquake rupture variations to represent the conditional probability of future shaking at 285 geographic sites in the Los Angeles region (~236 million horizontal-component seismograms). This combination provides significant probability gains relative to OEF models based on empirical ground-motion prediction equations (GMPEs), primarily because the physics-based CyberShake simulations account for the rupture directivity, basin effects, and directivity-basin coupling that are not represented by the GMPEs.

Seismic shaking scenarios in realistic 3D basin model of Po Plain (Northern Italy), *Irene Molinari (INGV) and Andrea Morelli (INGV)*

Unexpected large and prolonged shaking (> 50s) associated with long-period ground motion has been observed inside the Po Plain sedimentary basin (Northern Italy) during the two M~6, May 20-29, 2012, earthquakes. Long-period ground motion mainly impacts on the seismic response of taller structures. It is hence important to understand the characteristics of long-period ground motion associated with the 3D structure and fault properties, in particular in those regions with deep sedimentary basins and a complex geological context.

We defined a three-dimensional model of the Po Plain basin by merging the abundant information existing in the form of borehole data and seismic reflection profiles that had been shot in the '70s and the '80s for hydrocarbon exploration. The final model is composed by seven laterally-varying layers, corresponding to the main geological units. In each layer we specify 1D velocity profiles for P-wave velocity, S-wave velocity, and density (Molinari et al., 2014). The model has been implemented in the spectral-element code SPECFEM3D_Cartesian (Peter et al., 2012) to simulate seismic waves. The simulations are numerically accurate for periods of 3 sec and longer, and incorporate complex 3D basin structure and topography. We show a preliminary validation of the model, trough visual comparison with recorded data, measuring on data and synthetics PGA/PGV, shaking duration, pseudo spectral accelerations, frequency contents, and historical data such as shake map and damage maps. Comparison with the predictions of a 1D model and a regional 3D model, EPcrust (Molinari & Morelli, 2011), will also be showed.

We evaluate ground motion produced by plausible earthquakes inferred from historical data, such as the Modena (1501) and Verona (1117) events that caused well-documented strong effects in a unusually wide areas with lengths of hundreds of kilometers.

Behavior of high-frequency seismic radiation, revealed by hybrid back-projection method, *Ryo Okuwaki, Yuji Yagi (U Tsukuba) and Shiro Hirano (U Tsukuba)*

High-frequency seismic waves are, in general, generated by an abrupt change of rupture velocity and slip-rate (e.g., Spudich and Frazer, 1984). Therefore, analysis of high-frequency waves is of great importance to understand the dynamic rupture process of an earthquake. The hybrid back-projection (HBP) method (Yagi et al., 2012) is a tool to estimate the spatiotemporal distribution of high-frequency (0.5–2.0 Hz) sources by stacking the cross-correlation function of the observed waveform and the corresponding Green's function. Here we applied the HBP method to two great earthquakes; the Mw 8.8 2010 Maule Chile earthquake and the Mw 8.1 2014 Iquique Chile earthquake. We assumed a non-planar fault model that reflects the geometry of the slab surface (Tassara & Echaurren, 2012) to consider variations in focal mechanisms during rupture. To evaluate the relationship between high-frequency radiation and the dynamic rupture process, we compared the result with the spatiotemporal distribution co-seismic slip obtained by the novel waveform inversion technique developed by Yagi and Fukahata (2011).

In the 2010 Maule earthquake, we found that strong high-frequency radiation might be a precursory phenomenon that is a potential trigger of a large asperity rupture. Another important role of high-frequency radiation is that the weak high-frequency sources, distributed in-between the two large asperities near the hypocenter and the north of the hypocenter, might reflect the perturbation of rupture velocity and possibly bridge the two large-asperity ruptures.

In the 2014 Iquique earthquake, the spatiotemporal distribution of high-frequency radiation obtained by using the HBP method indicate following the complex rupture process; the initial rupture with southward

directivity for the first ~20 s, main rupture of large asperity that propagates bilaterally, and the northward back-propagating rupture to the hypocenter.

Thus, the spatiotemporal distribution of high-frequency sources obtained by using the HBP method can directly provide the image of complex rupture process and can be useful for source modeling by waveform inversion.

Postseismic deformation following the 2010 El Mayor-Cucapah earthquake: observations, kinematic inversions and endmember models, *Christopher Rollins (Caltech), Sylvain Barbot (Earth Observatory of Singapore) and Jean-Philippe Avouac (Cambridge University)*

Due to its location along a transtensional section of the Pacific-North American plate boundary, the Salton Trough is a region in which postseismic deformation may be supercharged. The extensional component of relative plate motion has created a regime of shallow asthenosphere and high heat flow that may feature reduced viscosities throughout the crust and upper mantle, while the transform component of relative plate motion creates large strike-slip earthquakes within this structure - potentially inducing significant viscoelastic relaxation - as well as a complex array of faults that may slip aseismically. The 2010 M=7.2 El Mayor-Cucapah earthquake was the largest shock in the Salton Trough since 1892 and occurred close to the U.S.-Mexico border, and so the postseismic deformation recorded by the continuous GPS network of southern California may provide insights into the rheology of this region. Three-year postseismic transients extracted from GPS displacement timeseries show four key features: 1) 1-2 cm of cumulative uplift in the Imperial Valley and ~1 cm of subsidence in the Peninsular Ranges, 2) relatively large cumulative horizontal displacements >150 km from the rupture in the western Peninsular Ranges, 3) rapidly decaying horizontal displacement rates in the first few months after the earthquake in the Imperial Valley, and 4) more sustained horizontal velocities, following the rapid early motions, that were still visibly ongoing three years after the earthquake. Kinematic inversions show that the cumulative three-year postseismic displacement field can be well fit by afterslip on the coseismic rupture. Forward modeling shows that stress-driven afterslip in the lower crust and Yuha Desert can reproduce the rapidly decaying early horizontal velocities in the Imperial Valley, and afterslip extending into the upper mantle with different frictional parameters can reproduce the sustained horizontal velocities following them. We find that Newtonian viscoelastic relaxation in the lower crust and possibly the mantle lithosphere can also reproduce the sustained horizontal motions in the Imperial Valley, while viscoelastic relaxation with a stress-dependent rheology in the lower crust and possibly the mantle lithosphere can reproduce the rapidly decaying early velocities there. We find that Newtonian viscoelastic relaxation in the asthenosphere can reproduce the uplift in the Imperial Valley and the subsidence and large westward displacements in the Peninsular Ranges. We present two forward models of dynamically coupled deformation mechanisms that fit the postseismic transient well: a model combining afterslip in the lower crust and Yuha Desert, Newtonian viscoelastic relaxation in a localized zone in the lower crust consistent with high heat flow and geothermal areas, and Newtonian viscoelastic relaxation in the asthenosphere; and a second model that replaces the afterslip in the first model with viscoelastic relaxation with a stress-dependent rheology in the mantle. The rheology of this high-heat-flow, high-strain-rate region may incorporate elements of both these models and may be well more complex than either of them.

Monitoring of microseismicity in Japan by applying the matched filter technique to Hi-net continuous records, *Kaoru Sawazaki (NIED)*

Due to the overlap of seismic coda waves and aftershocks in seismograms, detection of small earthquakes by hand-picking is very difficult after a large earthquake. In Japan, even though the JMA (Japan Meteorological Agency) unified hypocenter catalog has detected down to M1 earthquakes occurring in inland Japan, there are still many missing smaller events especially after large earthquakes. In such situation, alternatively, the Matched Filter (MF) technique which uses similarity of waveform pair has been widely applied. If the correlation coefficient (CC) between seismograms of two events is large and source parameters of one of the two events have been identified, another event would share the same source location, source mechanism, and propagation path. In this study, I use the Hi-net records of already identified earthquakes as templates, and detect as many similar events as possible by applying the MF technique to the Hi-net continuous records.

The template events must satisfy the following conditions;

1. M≦2.0
2. Less than 10km to the closest Hi-net station
3. Shallower than 20km depth
4. S/N must be over 10

I select 305,053 template events which satisfied above conditions from October 2000 to June 2014. Applying 3-30Hz bandpass filter to up-down component of Hi-net records, I make template waveforms. Then I compute CC between the template waveform and the continuous Hi-net records, and pick up the traces if their CC exceeds 0.8.

So far, the computation has been finished for seven years. The number of detected events is several times greater than that listed in the JMA unified hypocenter catalog. The detection improvement is especially fine after large earthquakes. If we look at an example of the 2000 Western Tottori earthquake (M6.8), the location

of newly detected earthquakes is localized along east-westward, where similar aftershocks could be occurring repeatedly due to post-seismic deformation. The database of the MF-based catalog would be used for many objectives, such as mapping of cumulative slip, time-lapse monitoring of seismic velocity, and so on.

Stochastic descriptions of small-scale, near-surface velocity variations in the Los Angeles basin, *Xin Song (USC), Thomas H. Jordan (USC), Andreas Plesch (Harvard) and John H. Shaw (Harvard)*

SCEC has completed Phase 1 of its Broadband Platform (BBP) ground motion Simulations of earthquake ground motions at high frequencies (> 1 Hz) require high-resolution velocity models to quantify the effects of wave scattering, attenuation, and anisotropy. Valuable information about the statistical variations of the velocity structure in the upper few kilometers of the crust can be obtained from well logs. We apply geostatistical methods to characterize the one-point and two-point statistics of velocity variations observed at vertical scale lengths less than 200 m in an ensemble of vertical sonic logs from the central Los Angeles basin. The stochastic variability at these scales can be separated into two components, one with a correlation length of about 10-60 m and a second with a correlation length of about 1-4 m. The one-point statistics of both components are distinctly non-Gaussian, with those of the first skewed to low velocities and those of the second skewed to high velocities. Assuming that the horizontal correlation lengths are much greater than the vertical correlation lengths, we then obtain a long-wavelength polarization anisotropy of around 6-8% from up-scaling method of the profiles. We also investigate the magnitude of wave scattering caused by the small-scale heterogeneity and speculate on its role in explaining the anomalous near-surface attenuation of high-frequency seismic waves.

Inversion for the physical parameters that control the source dynamics of the 2004 Parkfield earthquake, *C. Twardzik (UCSB), R. Madariaga (ENS Paris), and S. Das (U of Oxford)*

A fully dynamic inversion for the earthquake source process, in which the geometry of the rupture area, the stress conditions, and frictional properties on the fault are obtained, is carried out by inverting displacement records for the 2004 Mw6.0 Parkfield, California, earthquake. The rupture area of the earthquake is modeled using elliptical patches, and seismograms from 10 near-field digital stations

are used. Synthetic tests to investigate the performance of the inversion in retrieving the rupture process demonstrate that we can reliably recover the large scale features of the spatiotemporal distribution of slip. To investigate the stress conditions and frictional properties of the fault under which we produce a rupture model that fits the observed data, we explore the parameter space using a Monte Carlo method and find an optimal region where the source models fit the data well. The best fitting rupture process is shown to occur mainly within one horizontal elliptical region, 22 km long along strike and 4 km wide along depth. The seismic moment is 1.2 x 1018 Nm, and the stress drop over the ellipse is ~4 MPa. The rupture speed, nearly constant during the entire rupture process, is ~2.9 km/s. The dimensionless quantity k (roughly the strain energy change per unit fault surface divided by the energy release rate), which includes information on the stress and frictional properties on the fault, is found to be ~1.4 for the ellipse and strongly controls the rupture process along with the size of the initial circular patch that initiates the earthquake.

The site attenuation parameter in New Zealand and its variability, *Chris Van Houtte (University of Auckland), Caroline Holden (GNS Science), Tam Larkin (University of Auckland) and Olga Ktenidou (ISTerre)*

The site attenuation parameter, κ_0, is an important parameter in rock-site ground-motion prediction, and is included in multiple ground-motion prediction frameworks such as stochastic simulations and ground-motion prediction equation (GMPE) adjustments. Recently, it has been suggested that considering κ_0 in empirical GMPEs may improve rock-site predictions. Before κ_0 can be reliably used in forward prediction, its behaviour must be well-defined in its intended region of application. This study presents κ_0 values for 34 rock-sites in GeoNet's New Zealand National Seismic Network, and compares these values with local geology, tectonic setting and previous *Q* attenuation studies. κ_0 in the low-to-moderate seismicity Otago region of New Zealand ranges from 0.004 – 0.010 s, while values in the active East Coast subduction forearc range from 0.038 – 0.058 s. The aleatory uncertainty of the κ_0 data is also quantified, and it is demonstrated that existing calculations of uncertainty in κ_0 for regional reference rock site conditions do not fully capture the total aleatory uncertainty in κ_0.

Long-Period Ground Motion Simulations for Subduction Earthquakes Using the Ambient Seismic Field, *Loic Viens (ERI), Kazuki Koketsu (ERI), and Hiroe Miyake (ERI)*

Ground motion prediction is critical to evaluate the seismic hazard specially in high seismicity areas as Japan. We focus this study on long-period ground motions which can significantly affect large-scale structures having a long-period resonance such as high-rise buildings, bridges, or oil tanks. We used deconvolution method without any pre-processing to extract reliable phase and amplitude of single force impulse response function between two stations from the ambient seismic field. This method allows to predict accurate ground motions at periods longer than 4 s for moderate earthquakes without the need of any external information about the velocity structure. However, only relative, rather than absolute, amplitudes can be recovered. To retrieve corresponding Green's functions, impulse response amplitudes need to be calibrated using records of an earthquake which happened close to the "virtual" source. Moreover, as surface-to-surface Green's functions are extracted, some mismatches are observed between Green's functions and the earthquake records. This feature is due to the fact that depth and focal mechanism of the event are not taken into account. We first

used this technique in the Tokai/Tonankai subduction zone and we extracted Green's functions between seismic stations located on the ocean bottom and on-land Hi-net stations. We validate this approach by comparing computed Green's functions with offshore moderate earthquake (M_w ~5) records in the Nobi sedimentary basin where the Nagoya city is located. Then, we extracted Green's functions between Hi-net stations located above the 1923 Kanto earthquake fault that we considered as "virtual" sources and Hi-net stations located in the Kanto basin. We also validate this approach by comparing Green's functions with real moderate earthquakes (M_w ~5) which can be treated as point sources at the wavelengths/periods of interest. Finally, we apply the method developed by Denolle et al. (2014) to extend from point sources to a finite rupture of M_w ~7 earthquakes using the representation theorem. These results are finally compared to long-period ground motion prediction equations to evaluate their validity.

The M9 Project and probabalistic modeling of megathrust events in Cascadia: An Overview, *Erin A. Wirth (U Washington)*

The M9 Project is a large-scale, multidisciplinary study that aims to reduce the catastrophic potential of a megathrust earthquake (i.e., of Magnitude 9) in Cascadia. This will be accomplished by integrating modeling of seismic events and subsequent hazards (e.g., tsunamis, liquefaction, and landslides) with advances in earthquake early warning and adaptive community planning. In order to better inform early warning and community resilience studies, the M9 project will focus on probabilistic predictions of a M9 event and its associated hazards, as opposed to relying on a few generalized scenarios.

A significant portion of the M9 project depends upon the character of strong ground motions produced by a megathrust event. Many previous studies have used average predicted values of shaking based on a location's distance from the rupture. While valuable, this assumes that shaking is identical along the rupture zone given a certain magnitude, distance, and site condition. Damage calculations do not always take into account factors such as the duration of shaking, directivity of the rupture, or amplification from sedimentary basins, all of which are critical in evaluating building response and the potential for liquefaction and landslides. Therefore, simulations utilizing a 3-D geologic model are necessary in order to accurately characterize the destructive power of seismic ground motions. By running an ensemble of simulations, the M9 project aims to capture the variability of ground motions such that probabilistic estimates of a M9 earthquake in Cascadia can be determined. Ultimately, the resulting seismograms and ground motions, along with their associated probabilities and uncertainties, will be used to inform community-based scenario planning and warning systems.

High-Complexity Deterministic Q(f) Simulation of the 1994 Northridge Mw 6.7 Earthquake, *Kyle B. Withers (SDSU/UCSD), Kim B. Olsen (SDSU), Zheqiang Shi (SDSU), and Steve Day (SDSU)*

With the recent addition of realistic fault topography in 3D simulations of earthquake source models, ground motion can be deterministically generated more accurately up to higher frequencies. The synthetic ground motions have been shown to match the characteristics of real data, having a flat power spectrum up to some cutoff frequency (Shi and Day, 2013). However, the earthquake source is not the only source of complexity in the high-frequency ground motion; there are also scattering effects caused by small-scale velocity and density heterogeneities in the medium that can affect the ground motion intensity. Here, we dynamically model the source of the 1994 Mw 6.7 Northridge earthquake using the Support Operator Rupture Dynamics (SORD) code up to 8 Hz. Our fault model was input into a layered velocity structure characteristic of the southern California region characterized by self-similar roughness from scales of 80 m up to the total length of the fault. We extend the ground motion to further distances by converting the output from SORD to a kinematic source for the finite difference anelastic wave propagation code AWP-ODC. This code incorporates frequency-dependent attenuation via a power law above a reference frequency in the form Q0fn.

We model the region surrounding the fault with and without small-scale medium complexity, with varying statistical parameters. Furthermore, we analyze the effect of varying both the power-law exponent of the attenuation relation (n) and the reference Q (Q0) (assumed to be proportional to the S-wave velocity), and compare our synthetic ground motions with several Ground Motion Prediction Equations (GMPEs) as well as observed accelerograms. We find that the spectral acceleration at various periods from our models are within 1 interevent standard deviation from the median GMPEs and compare well with that of recordings from strong ground motion stations at both short and long periods. At periods below 1 second, Q(f) is needed to match the decay of spectral acceleration seen in the GMPEs as a function of distance from the fault (n~0.6-0.8).We find when binning stations with a common distance metric (such as Joyner-Boore or rrup) that the effect of media heterogeneity is canceled out, however, the similarity between the intra-event variability of our simulations and observations increases when small-scale heterogeneity is included.

An improved method to calculate normal mode of a semi-closed bay or ocean basin, *Yifei Wu (ERI) and Kenji Satake (ERI)*

Normal mode calculation of a semi-closed or completely closed bay or ocean basin is an important topic because it helps us to understand the oscillation characteristics including those excited by incoming tsunamis. In addition, tsunami propagation can be synthesized by superposition of normal modes.

Starting from Laplace's tidal equations and ignoring the rotation of the earth, Loomis (1975) discretized the problem into the eigenvalue problem of a symmetric sparse matrix, which was solved by Householder

transformations. This method is used by Satake and Shimazaki (1988) for Japan Sea and Aida (1996) for Tokyo Bay. However, this method needs O(n^3) operation in time and O(n^2) in memory (n is the total number of water grid. e.g., for Japan Sea in 30 sec grid, n~10^6), which would require a super computer.

To overcome this disadvantage, we first introduce a recent iteration method called Implicitly Restarted Arnoldi Method (Lehoucq et al., 1997), which itself speeds up the calculation a bit. Then after we develop a sparse version of matrix storage and multiplication, the operation count in time and memory reduced dramatically to O(n^1.5) (including about 0.5 for iteration process) and O(n) respectively, utilizing the special property of the matrix and the iteration method. This means any current computer can easily solve a large eigenvalue problem.

Recent methods to calculate normal mode of global ocean (e.g., Muller, 2007) consider additional factors than the presented one, while complicated program and far more computing resources are required.

The spatial variation of tidal sensitivity of tectonic tremor, *Suguru Yabe (EPS/U Tokyo), Satoshi Ide (EPS/U Tokyo), Yoshiyuki Tanaka (ERI/U Tokyo), Heidi Houston (UW)*

Tectonic tremor, which is part of “slow earthquake”, has been detected in many subduction zones and transform faults. It has been known that various quantities characterizing tectonic tremors vary among subduction zones and even within the individual subduction zone. The heterogeneity in such tremor characteristics should reflect the heterogeneity of frictional behavior on the subducting plate interface. To understand such heterogeneity on the plate interface and the mechanism generating slow earthquake, we have investigated the spatial variation of tectonic tremor activities. So far, we have investigated the spatial variation of duration, recurrence interval, and the amplitude (seismic energy rate) of tremors (Ide, 2012; Idehara et al., 2014; Yabe and Ide, in revision). As a next step, we started investigating the spatial variation of tidal sensitivity of tremors in Nankai and Cascadia subduction zones.

Both body tide and ocean tide are included in the calculation of tidal stress. We calculated Green functions for the spherical Earth based on the method by Okubo and Tsuji (2001). The time history of sea surface level is calculated with the SPOTL program (Agnew, 2012). The fault planes of VLF estimated by Ide and Yabe (2014) and a slab model constructed by Hayes et al. (2012) are used to calculate stress on the plate interface.

We compare the time series of calculated tidal shear stress with the tremor catalog. Tremors are more likely to occur when tidal shear stress is larger, in the subduction direction. Tremor rate appears to increase exponentially with tidal shear stress, as previously seen by Houston (2013, AGU). In the inter-ETS activity, some regions where tremor amplitude is small show tidal sensitivity. In the ETS activity, tidal sensitivity can be seen clearly during the later portions of large SSEs, consistent with behavior reported by Houston (2013, AGU). In the regions where tidal sensitivity can be seen, the rake direction of VLF is consistent with the direction of maximum tidal shear stress on that fault plane. This observation might imply that tidal stress significantly modulates the timing of slow slip on the deep plate interface.

A stress-field orientation in northwestern area of the Kanto plain, Japan, *Tomoko E. Yano (NEID), Tetsuya Takeda (NEID), Katsuhiko Shiomi (NEID)*

Tectonic tremor, which is part of “slow earthquake”, has been detected in many subduction zones and transform faults. It has been known that various quantities characterizing tectonic tremors vary among subduction zones and even within the individual subduction zone. The heterogeneity in such tremor characteristics should reflect the heterogeneity of frictional behavior on the subducting plate interface. To understand such heterogeneity on the plate interface and the mechanism generating slow earthquake, we have investigated the spatial variation of tectonic tremor activities. So far, we have investigated the spatial variation of duration, recurrence interval, and the amplitude (seismic energy rate) of tremors (Ide, 2012; Idehara et al., 2014; Yabe and Ide, in revision). As a next step, we started investigating the spatial variation of tidal sensitivity of tremors in Nankai and Cascadia subduction zones.

Rupture Characteristics of Large (Mw ≥ 7.0) Megathrust Earthquakes from 1990-2014, *Lingling Ye (UCSC), Thorne Lay (UCSC) and Hiroo Kanamori (Caltech)*

Seismic wave radiation from megathrust earthquakes provides an important probe of fault zone properties and interplate rupture attributes. Depth-varying rupture characteristics of short-period seismic radiation for earthquakes along megathrusts have been inferred from several recent giant earthquakes and large tsunami earthquakes. To quantify any depth-dependent variations more extensively, we performed systematic analysis of 112 $M_w \geq 7.0$ thrust-faulting earthquakes on circum-Pacific megathrust faults using teleseismic body wave finite-fault inversions and source spectrum determinations. Large tsunami earthquakes and some other shallow events at depths less than about 18 km have unusually long source durations, low static stress drops and strongly depleted short-period radiation. Deeper events have no clear trend with source depth for moment-normalized centroid duration, static stress drop, moment-scaled total radiated energy, apparent stress, or radiation efficiency. Scaling with seismic moment supports self-similarity for several source characteristics for the large earthquake population, albeit with substantial scatter. However, the source spectra have high-frequency spectral decay slopes averaging ~-1.6, rather than -2, the expected value for a standard ω^{-2} model. This may result from compound nature of large megathrust ruptures with varying scale lengths of heterogeneity, but is also influenced by attenuation assumptions. There is relative enrichment in short-period spectral levels with increasing depth manifested in reduced high-frequency spectral decay slope.

The ratio of high-frequency (0.3-1Hz) radiated energy to total energy increases correspondingly. Radiation efficiency tends to decrease with average slip for the large events, and estimates of fracture energy increase steadily with slip. Correlation of higher estimated average megathrust temperature at 30 km depth with higher spectral decay rate indicates that the depth-varying pattern may in part result from frictional properties being influenced by temperature variations or from a systematic reduction of average attenuation with increasing depth along the megathrust.

Notes

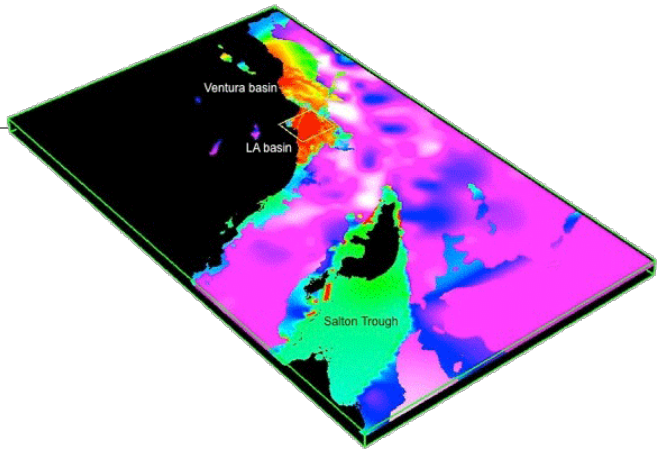

Notes

The SCEC Broadband Platform

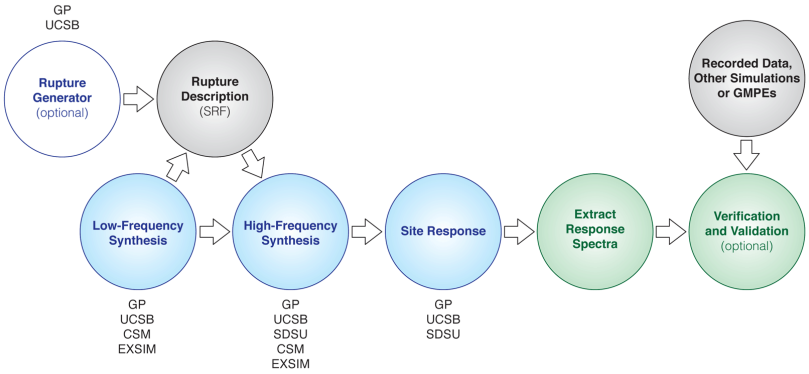

The SCEC Broadband Platform integrates various simulation and processing software tools into a system that supports easy on-demand computation of broadband seismograms. The modules supported by the platform include rupture generators, low- and high-frequency ground motion simulators, non-linear site effects correctors, and visualization tools to facilitate verification and validation with data and ground motion prediction equations.

Notes

Loma Prieta Slip Distribution